

Research Paper

## The Integration and Functional Evaluation of Rabbit Pacing Cells Transplanted into the Left Ventricular Free Wall

Zhihui Zhang, Zhiyuan Song<sup>✉</sup>, Jun Cheng, Yaoming Nong, Lu Wei, Changhai Zhang

Department of Cardiology, Southwest Hospital, The Third Military Medical University; Interventional Cardiology Institute of Chongqing, Chongqing 400038, China.

✉ Corresponding author: Zhiyuan Song, Department of Cardiology, Southwest Hospital, The Third Military Medical University; Interventional Cardiology Institute of Chongqing, Chongqing 400038, China. Tel: +86-023-68765168; Fax: +86-023-68765168; E-Mail: zhiyuan.song@public.cta.cq.cn.

© Ivyspring International Publisher. This is an open-access article distributed under the terms of the Creative Commons License (<http://creativecommons.org/licenses/by-nc-nd/3.0/>). Reproduction is permitted for personal, noncommercial use, provided that the article is in whole, unmodified, and properly cited.

Received: 2012.08.01; Accepted: 2012.08.20; Published: 2012.08.27

### Abstract

To evaluate the feasibility of cell transplantation to treat bradyarrhythmia, we analyzed the *in vivo* integration and pacing function after transplantation of mHCN4-modified rabbit bone marrow mesenchymal stem cells (MSCs) into the rabbit left ventricle free wall epicardium. In our investigation, we injected MSCs transduced with or without mHCN4 into the rabbit left ventricle free wall epicardium. Chemical ablation of the sinoatrial node was performed and bilateral vagus nerves were sequentially stimulated to observe premature left ventricular contraction or left ventricular rhythm. We found that the mHCN4-transduced MSC group had a significantly higher ventricular rate and a shorter QRS duration than that of the control and EGFP group. Furthermore, the mHCN4-transduced MSCs, but not the control cells, gradually adapted long-spindle morphology and became indistinguishable from adjacent ventricle myocytes. The modified MSCs showed pacing function approximately 1 week after transplantation and persisted at least 4 weeks after transplantation. In conclusion, a bradyarrhythmia model can be successfully established by chemical ablation of the sinoatrial node and sequential bilateral vagus nerve stimulation. The mHCN4-modified rabbit MSCs displayed evident dynamic morphology changes after being transplanted into rabbit left ventricle free wall epicardium. Our studies may provide a promising strategy of using modified stem cell transplantation to treat bradyarrhythmia.

Key words: mHCN4, bone marrow mesenchymal stem cell, subepicardial transplantation, biological pacing.

### Introduction

Hyperpolarization activated cyclic nucleotide gated cation channels (HCN) are voltage-gated ion channels that structurally resemble K<sup>+</sup> channels, with a six-transmembrane domain topology, including a pore region that conducts ion flow[1]. HCN channels are encoded by four separate genes, HCN1-4, which are crucial for a range of electrical signalling, including cardiac and neuronal pacemaker activity [2-3]. In mammals' sinoatrial node, they are the molecular

basis of pacemaker current (I<sub>f</sub>), the presence of HCN1 and HCN4 isoforms has been verified in human sinoatrial node cells [4-6].

HCN genes are becoming important candidate genes in investigations using biological pacemakers to treat bradyarrhythmia, which were based on gene therapy and cell transplantation techniques [7-10]. In cloned 4 HCN gene subtypes, HCN4 is mainly expressed in the cardiac specific conduction system

[11-15]. Previously, 3 degree atrioventricular block models by radiofrequency catheter were established on a large animal model like dogs or pigs, and HCN2 was the target gene [14, 16-17]. In this study, we established a rabbit bradyarrhythmia model based on chemical ablation of the sinoatrial node and sequential bilateral vagus nerve stimulation, and evaluated the integration and pacing function after mHCN4-modified rabbit BMSCs were transplanted into left ventricle epicardium [18-20]. This study provides new insights and methods to explore biological pacing therapy.

## Materials and Methods

### Preparation of transplanted cells and electrophysiology analyses

BMSCs were separated and purified with Percoll separating medium by density gradient centrifugation and adherence method. Bone marrow was obtained from 2 month-old Japanese white rabbits (Experimental Animal Center, The Third Military Medical University) via intertrochanteric aspiration under aseptic conditions and washed twice by Percoll density gradient centrifugation (2,000 rpm for 10 minutes and 1,000 rpm for 10 minutes). The monocytes in middle white cloudy layer were harvested and washed twice with DMEM (GIBCO, USA) at 1,000 rpm for 5 minutes. Cells were cultured and propagated in DMEM containing 10% fetal bovine serum (Hyclone, USA) at a concentration of  $10 \times 10^8$ /ml. Transduction and antibiotic selection were performed using established methods in our lab [15]: Rabbit MSCs ( $p=4$ ) were plated into a 24-well plate at  $2 \times 10^4$ /well, a supernatant containing pMSCV-mHCN4-EGFP virus was mixed with medium at 1:1 and added into rabbit MSCs together with polybrene (Sigma, USA) at a final concentration of 2  $\mu$ g/ml. Twenty-four hours after transduction puromycin at 2  $\mu$ g/ml (Sigma, USA) was added and cells were selected for 10~15 days to get transduced rabbit MSCs. Immunofluorescence was used to determine the gene expression level in the control group, EGFP group, and mHCN4 group. Cells were prepared at a suspension of  $1 \times 10^6$  cells/ml and incubated on ice less than 5 minutes before injection.

Patch clamp was used to detect If and the activation curve 10 days after antibiotic selection. The intracellular solution (mmol/l) was as follows: KOH 146, NaCl 10, CaCl<sub>2</sub> 2.0, EGTA-KOH 5, Mg-ATP 2, HEPES-KOH 10, pH 7.2. Extracellular fluid (mmol/l) was: NaCl 140, NaOH 2.3, MgCl<sub>2</sub> 1.0, KCl 5.4, CaCl<sub>2</sub> 1.0, HEPES 5, glucose 10, aspartic acid 130, pH 7.4. Sealing resistance was more than 1.0 G $\Omega$ ; clamping

voltage was -40 mV; reference potential was -140~-40 mV; step voltage was 10 mV; pulse width was 4,000 ms.

### In vivo animal experiments and electrocardiogram

Forty-eight male and female 2 month-old Japanese white rabbits, 1.8~2.5 kg, were randomized into a control group ( $n=8$ , microinjected with 0.2 ml medium), EGFP group ( $n=20$ , injected with 0.2 mL pMSCV-EGFP transduced cell suspension), and mHCN4 group ( $n=20$ , injected with 0.2 mL pMSCV-mHCN4-EGFP transduced cell suspension). Animals were general anesthetized by 3% sodium pentobarbital (30 mg/kg via ear vein), and marked with 5-0 blue prolene sutures (Ethicon, USA) on the left ventricle free wall after median sternotomy to mark the injection region. The needle was inserted 2~3 mm at an angle of 30° in the adjacent site with a microsyringe, and 0.2 mL allochthonous cell suspension was injected into epicardium at two sites after aspiration without blood. At 3 days, 1 week, 2 weeks and 4 weeks after transplantation, 2, 5, 5 rabbits were selected from each respective group and bilateral neck vagus nerves were separated under anesthesia. After chemical ablation of the sinoatrial node, bilateral vagus nerves were sequentially stimulated to create a bradyarrhythmia model (stimulation voltage 4~6 V, stimulation frequency 10~20 Hz). Premature left ventricular contraction or left ventricular rhythm was determined. After that, tissues were harvested through thoracotomy. Body surface electrocardiogram (ECG) was recorded throughout the experiments (RM6280C Multichannel electrophysiology signal acquisition system, Chengdu Instruments, Sichuan).

### Histology and immunofluorescence

Tissues were fixed with 4% PFA, paraffin embedded, and sectioned. Sections were stained with HE or DAB staining. Cryosections were used for immunofluorescence. Primary antibodies used include monoclonal rat anti-mouse HCN4 (1:1000, Abcam, USA), and polyclonal goat anti-rabbit connexin-43 (1:200, Santa Cruz, USA). Secondary antibodies used include phycoerythrin labeled goat anti-rat IgG (1:200, Abcam, USA), and donkey anti-goat IgG (Abcam, USA). Normal rabbit ventricular myocytes were used as positive control, and PBS was used as negative control in place of a primary antibody.

### Statistical Analyses

All data was presented as mean  $\pm$  SD. T test and ANOVA analyses were performed with SPSS 10.0

software,  $P < 0.05$  was considered significant.

## Results

### Measurement of pacemaker current and activation curve in transduced cells

Time and voltage dependent hyperpolarization activated inward current could be detected in MSCs transduced with mHCN4, with an average current density of  $-42.6 \pm 3.8 \text{ pA/pF}$  under a reference voltage of  $-140 \text{ mV}$  (Fig. 1A). In contrast, no evident hyperpolarization activated inward current could be detected in the EGFP group (Fig. 1B). Apparent tail current could be detected when reference voltage depolarized to  $+20 \text{ mV}$  (Figure. 1C). Using reference voltage as the horizontal axis and normalized tail current intensity ( $\text{pA/pF} // \text{pA/pFmax}$ ) as the vertical axis, the mHCN4 channel activation curve was plotted (Fig. 1D). The half maximal activation voltage was  $-97.8 \pm 5.3 \text{ mV}$ , activation potential was  $-62.5 \text{ mV}$ .

### In vivo experiments and electrocardiogram

One rabbit from the EGFP group and 1 from the mHCN4 group died at 5 days and 18 days after transplantation, respectively, and experiments of the remaining 46 rabbits were successful. No significant difference in ventricular escape rhythm was observed after chemical ablation of the sinoatrial node and se-

quential bilateral vagus nerve stimulation among the three groups at 3 days after transplantation. At 1 week after transplantation, only one rabbit in the mHCN4 group had a ventricular rhythm higher than the control group or EGFP group (Fig. 2). However, the mHCN4 group had significantly higher ventricular rhythm ( $p < 0.01$ ) and shorter QRS duration ( $p < 0.05$ ) than the control or EGFP group, respectively (Table 1).

**Table 1** Ventricular rhythm and QRS duration at 2 weeks after transplantation (mean  $\pm$  SD). Compared to control group, \*:  $p < 0.01$ , \*\*:  $p < 0.05$ ; Compared to EGFP group,  $\Delta$ :  $p < 0.01$ ,  $\Delta\Delta$ :  $p < 0.05$ .

	Heart rate at 2 weeks (beat/min)	Heart rate at 4 weeks (beat/min)	QRS at 2 weeks (ms)	QRS at 4 weeks (ms)
Control group	66 $\pm$ 8	67 $\pm$ 9	145 $\pm$ 12	143 $\pm$ 11
EGFP group	68 $\pm$ 5	63 $\pm$ 6	142 $\pm$ 9	140 $\pm$ 10
mHCN4 group	93 $\pm$ 9 $\Delta$	91 $\pm$ 8 $\Delta$	120 $\pm$ 11 $\Delta\Delta$	121 $\pm$ 13 $\Delta\Delta$

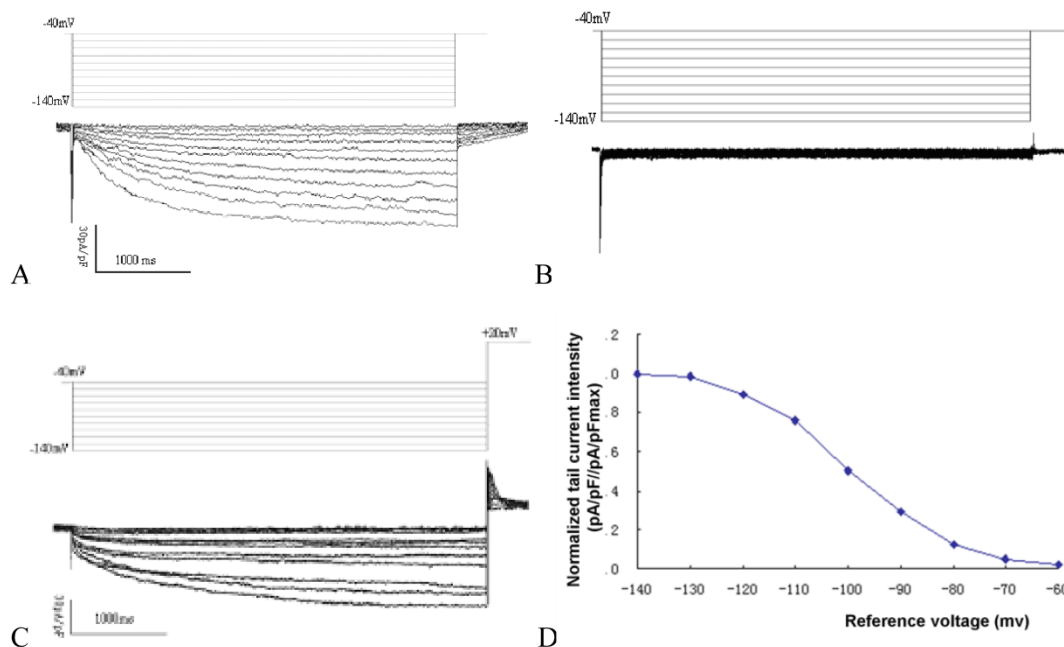


**Figure 1** A: If curve of cells in the mHCN4 group; B: No If can be detected in cells of the EGFP group; C: Tail current in mHCN4 cells when polarized to  $+20 \text{ mV}$ ; D: If activation curve in mHCN4 cell.

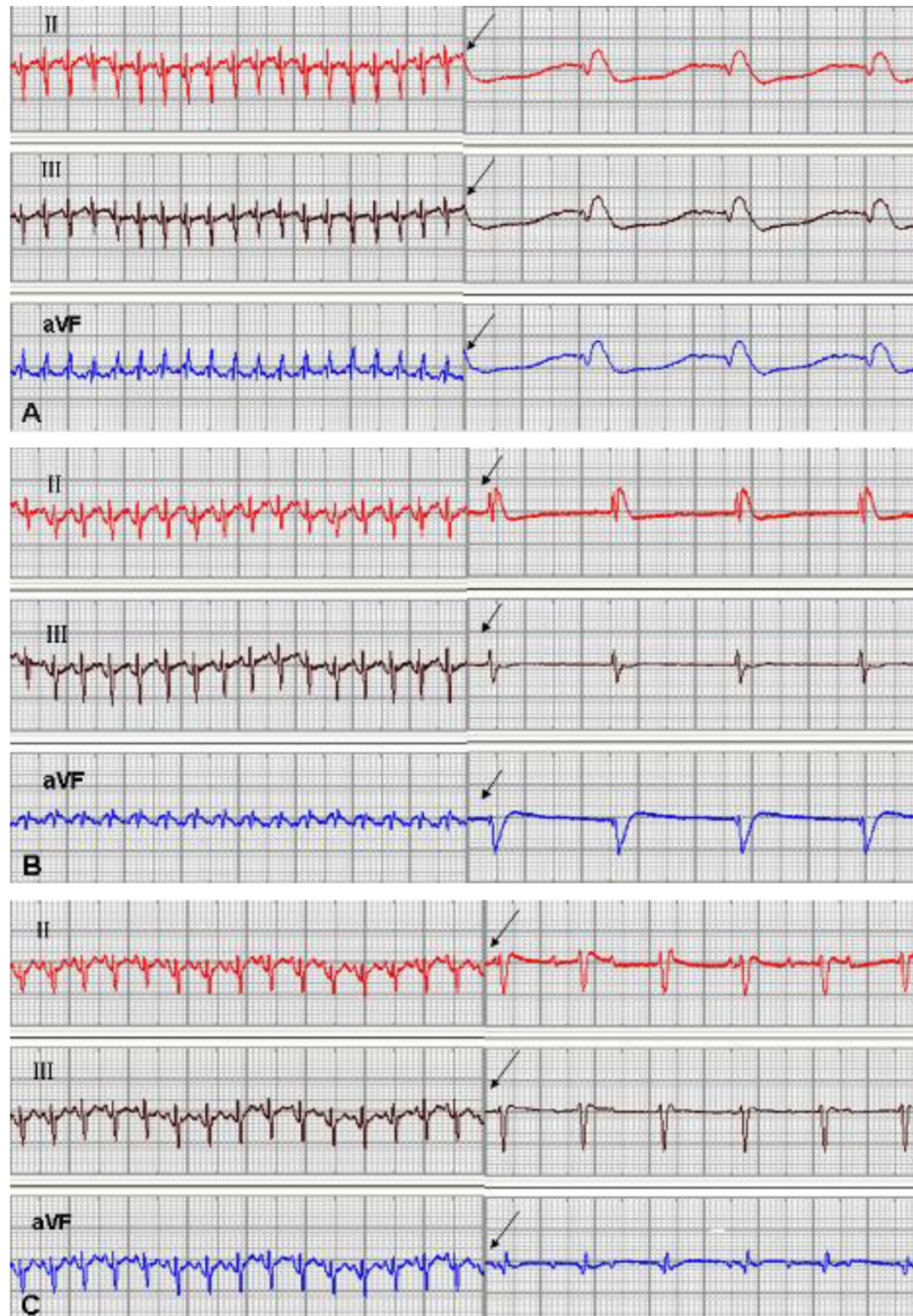


**Figure 2** Sinus rhythm and ventricle rhythm (arrow) after vagal nerve stimulation at 2 weeks after transplantation; A: control group, B: EGFP group, C: mHCN4 group (chart drive speed was 25 mm/s).

### HE and DAB staining

Morphology of the transplanted cells dynamically changed as observed by HE staining over time: At 3 days after transplantation, transplanted cells were round and clustered and had well-defined boundaries separating them from the adjacent normal ventricle myocytes (Fig. 3A). At 1 week after trans-

plantation, the cells decreased significantly, and short spindle cells could be observed in the region adjacent to the normal ventricle myocytes (Fig. 3B). At 2 weeks after transplantation, the transplanted cells displayed gradual transition to the adjacent ventricle myocytes and spindle cells increased (Fig. 3C). At 4 weeks after transplantation, the surviving transplanted cells were in long-spindle morphology and could not be clearly

discriminated from adjacent ventricle myocytes (Fig. 3D). In the control group, mild inflammation was observed in the transplanted region as determined by HE staining after medium injection, and no dynamic

changes were observed. Cx43 and Cx45 could be detected between transplanted cells and host cells by DAB staining, which were brown linear granulates (Fig. 4).

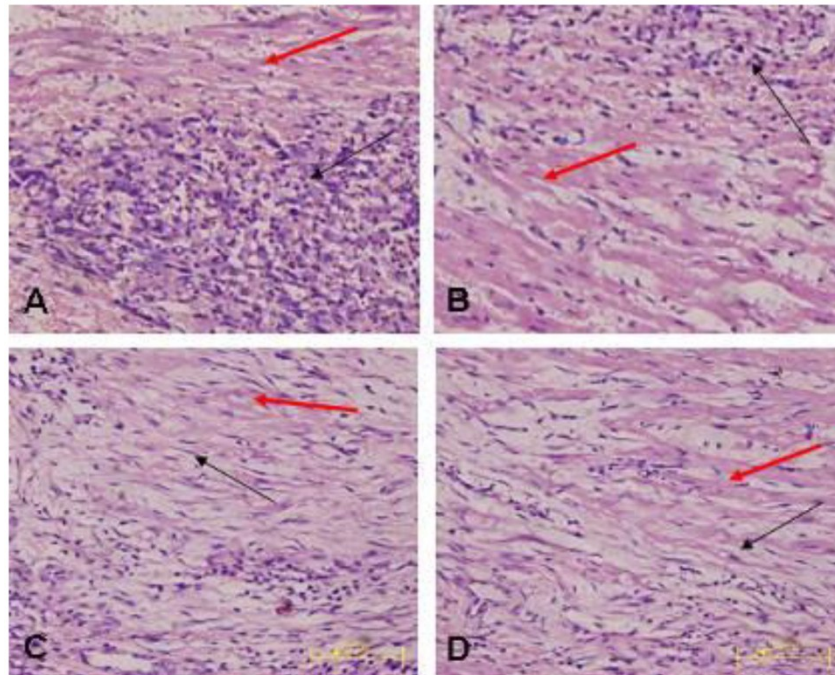


**Figure 3** Transplanted cells observed by HE staining (x400); black arrow indicates transplanted cells, red arrow indicates host ventricle myocytes. A: Three days after transplantation, B: One week after transplantation, C: Two weeks after transplantation. D: Four weeks after transplantation.

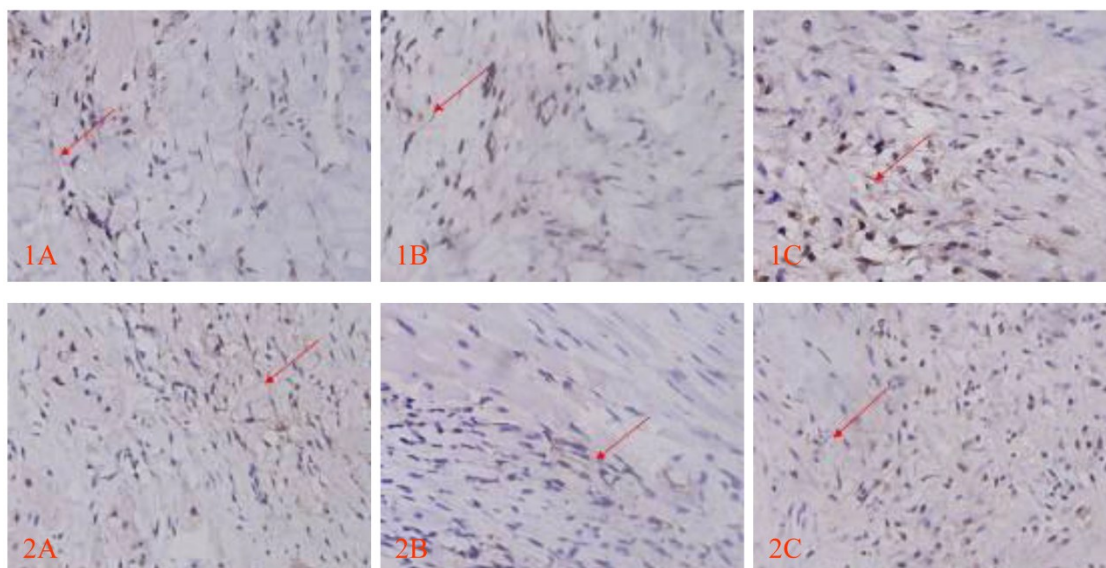


**Figure 4** Cx43 and Cx45 expression determined by DAB staining between transplanted cells and host cells; red arrow indicates positive signal, brown linear granulates (x400). 1: CX43, 2: CX45; A: Control group, B: EGFP group, C: EGFP-mHCN4 group.

### Immunofluorescence Results

EGFP and mHCN4 could be detected in the transplanted cells at 3 days after transplantation. The cells were round, not spread, and were negative for Cx43. One week after transplantation, surviving transplanted cells decreased, a few were short and spindle-like, and positive for EGFP, mHCN4, and

Cx43. Two weeks after transplantation, transplanted cells were long and spindle-like, with morphology similar to the adjacent ventricle myocytes. Cx43 could be detected between transplanted cells and host cells. Similar results could be observed 4 weeks after transplantation (Fig. 5).

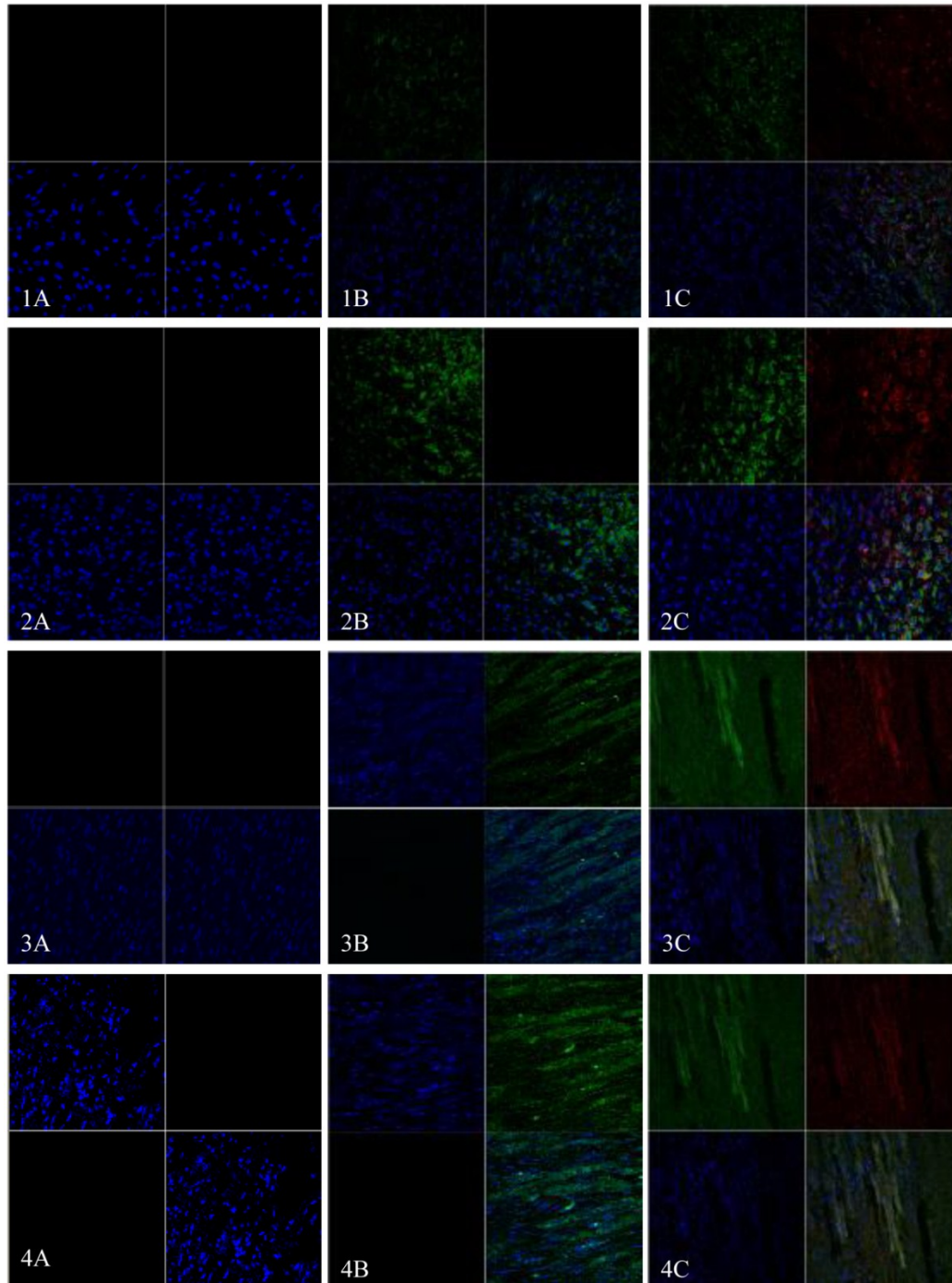


**Figure 5** Immunofluorescence of EGFP (Green) and mHCN4 (Red); nuclei were stained by DAPI (blue, x 400). 1: 3 days after transplantation, 2: 1 week after transplantation, 3: 2 weeks after transplantation, 4: 4 weeks after transplantation; A: control group, B: EGFP group, C: EGFP-mHCN4 group.

## Discussion

Many advances have been made in the biological pacing field, and a few attempts have been made on in vivo biological pacing. Various cells with high autorhythmicity combined with infectious solution were transplanted into the atrial/ventricle free wall or transduction bundle, with an atrioventricular block model by radiofrequency catheter; transplanted cells derived ectopic rhythm could be determined. Histology also detected gap junctions formed between transplanted cells and host cells [16, 21-22]. Most of these studies were performed on bradyarrhythmia created in large animal models, such as dogs or pigs, by radiofrequency catheter. This method requires advanced equipment, is difficult to manipulate, and not suitable for small animal models [14, 23]. Additionally, electronic cardiac pacemaker implantation was usually required to keep the animal alive, which made the experimental procedure more complex and increased the cost. The heart is controlled by vagus nerves on the left and right side. The most abundant site vagus nerve is located in the atrial node, the second in the atrioventricular node. Stimulation of the heart vagus nerve can induce a release of acetyl choline from the postganglionic neurofiber endings, which affect the cholinergic receptor on the atrial node, the atrioventricular node, or cardiomyocytes membrane, leading to negative chronotropic and dromotropic action. Stimulation on the right vagus nerve at a certain frequency can decrease the heart beat and even lead to asystole. Stimulation on the left vagus nerve usually slowed down atrioventricular conduction. Intense stimulation lead to ventricular block, even complete conduction block in the atrioventricular junction region. In vivo pacing experiments on rabbits can effectively reflect therapy, and make it relatively easy to perform surgery, feed, and observe after surgery. Due to the relatively higher basic heart rate, direct vagus nerve stimulation is not ideal. We first reduced the basic heart rate by chemical ablation of the sinoatrial node and then stimulated bilateral vagus nerves. This enabled us to analyze the pacing function of biological pacing cells during a ventricular block, and restore the sinus rhythm after observation. The animal can be fed for a long time without electronic cardiac pacemaker implantation. This model is relatively simple, costs little, is suitable for big and moderate animals, and is more versatile.

There is evidence that the transplanted cells began to die 1 day after transplantation. Scaling up the transplanted cells from 6 million to 25 million did not enlarge the transplantation area, due to the death of a majority of the transplanted cells. It is now thought

that the loss of transplanted cells can be attributed to two factors: The first one is a technical problem, and involves the cells remaining in the syringe, which leak into the ventricle chamber, pericardial cavity, vascular lumen or lymphatic system, and account for 45% of the total cells. The other one is cell death, which accounts for 50% to 75% of the total injection. Irreversible ischemic damage and apoptosis can be observed in dead cells under an electron microscope [24]. In this study, apparent aggregation of cell suspension could be observed in the epicardium when the injection volume reached 0.2ml. To reduce local tension, we did not inject the 1 ml that is usually used in studies. Transplanted cells formed a large aggregation in the transplanted region in tissue sections, and massive cell death could be found in the central region. Most of the surviving transplanted cells resided in a region adjacent to the normal ventricle myocytes, which may be due to the abundant cytokines and blood supply. We believe that greater injection volume is not better, as larger injection volume leads to higher tension, which can affect the survival rate of transplanted cells via dramatic changes of the microenvironment. Most of the injected cells died, and the surviving cells were those transplanted in regions adjacent to the normal ventricle myocytes. Therefore, small quantity and multi-site injection is beneficial for the survival of transplanted cells. Based on the dynamic changes of the transplanted cell morphology, the cells decreased in number as the shape changed gradually from round to spindle. After 2 weeks, most of the transplanted cells died and were absorbed, and the local damages induced by transplantation were largely repaired 2 weeks after transplantation. The surviving cells had similar morphology to the adjacent ventricle myocytes. Based on the gene expression and the function of transplanted cells, no significant difference in ventricular escape rhythm was observed among the 3 groups 3 days after transplantation. At 1 week after transplantation, only 1 rabbit in the mHCN4 group had a ventricular rhythm higher than the control group and EGFP groups. However, ventricular rhythm in the mHCN4 group was significantly higher than the control and EGFP groups at 2 weeks or 4 weeks after transplantation. Combined with the expression of gap junction proteins, we believe that transplanted cells were effective 2 weeks after transplantation.

## Acknowledgements

This work was supported by the National Natural Science Foundation of China (Grant No. 30871060) and the Chongqing Natural Science Foundation of China (No. 2008BA5005).

## Conflict of Interests

The authors have declared that no conflict of interest exists.

## References

- Altomare C, Terragni B, Brioschi C, Milanesi R, Pagliuca C, Viscomi C, et al. Heteromeric HCN1-HCN4 channels: a comparison with native pacemaker channels from the rabbit sinoatrial node. *J Physiol*. 2003; 549: 347-59.
- Robinson RB, Siegelbaum SA. Hyperpolarization-activated cation currents: from molecules to physiological function. *Annu Rev Physiol*. 2003; 65: 453-80.
- Zagotta WN, Olivier NB, Black KD, Young EC, Olson R, Gouaux E. Structural basis for modulation and agonist specificity of HCN pacemaker channels. *Nature*. 2003; 425: 200-5.
- Verkerk AO, van Borren MM, Peters RJ, Broekhuis E, Lam KY, Coronel R, et al. Single cells isolated from human sinoatrial node: action potentials and numerical reconstruction of pacemaker current. *Conf Proc IEEE Eng Med Biol Soc*. 2007; 2007: 904-7.
- Verkerk AO, Wilders R, van Borren MM, Peters RJ, Broekhuis E, Lam K, et al. Pacemaker current (I<sub>f</sub>) in the human sinoatrial node. *Eur Heart J*. 2007; 28: 2472-8.
- Chandler NJ, Greener ID, Tellez JO, Inada S, Musa H, Molenaar P, et al. Molecular architecture of the human sinus node: insights into the function of the cardiac pacemaker. *Circulation*. 2009; 119: 1562-75.
- Morris GM, Boyett MR. Perspectives -- biological pacing, a clinical reality? *Ther Adv Cardiovasc Dis*. 2009; 3: 479-83.
- Boink GJ, Seppen J, de Bakker JM, Tan HL. Biological pacing by gene and cell therapy. *Neth Heart J*. 2007; 15: 318-22.
- Rosen MR, Brink PR, Cohen IS, Robinson RB. Cardiac pacing: from biological to electronic ... to biological? *Circ Arrhythm Electrophysiol*. 2008; 1: 54-61.
- Rosen MR, Robinson RB, Brink PR, Cohen IS. The road to biological pacing. *Nat Rev Cardiol*. 2011; 8: 656-66.
- Brioschi C, Micheloni S, Tellez JO, Pisoni G, Longhi R, Moroni P, et al. Distribution of the pacemaker HCN4 channel mRNA and protein in the rabbit sinoatrial node. *J Mol Cell Cardiol*. 2009; 47: 221-7.
- Baruscotti M, Bucchi A, Viscomi C, Mandelli G, Consalez G, Gnecci-Rusconi T, et al. Deep bradycardia and heart block caused by inducible cardiac-specific knockout of the pacemaker channel gene Hcn4. *Proc Natl Acad Sci U S A*. 2011; 108: 1705-10.
- Potapova I, Plotnikov A, Lu Z, Danilo P, Jr., Valiunas V, Qu J, et al. Human mesenchymal stem cells as a gene delivery system to create cardiac pacemakers. *Circ Res*. 2004; 94: 952-9.
- Bucchi A, Plotnikov AN, Shlapakova I, Danilo P, Jr., Kryukova Y, Qu J, et al. Wild-type and mutant HCN channels in a tandem biological-electronic cardiac pacemaker. *Circulation*. 2006; 114: 992-9.
- Tong S, Yao Q, Wan Y, Zhou J, Shu M, Zhong L, et al. Development of functional I<sub>f</sub> channels in mMSCs after transfection with mHCN4: effects on cell morphology and mechanical activity in vitro. *Cardiology*. 2009; 112: 114-21.
- Plotnikov AN, Shlapakova I, Szabolcs MJ, Danilo P, Jr., Lorell BH, Potapova IA, et al. Xenografted adult human mesenchymal stem cells provide a platform for sustained biological pacemaker function in canine heart. *Circulation*. 2007; 116: 706-13.
- Kehat I, Khimovich L, Caspi O, Gepstein A, Shofti R, Arbel G, et al. Electromechanical integration of cardiomyocytes derived from human embryonic stem cells. *Nat Biotechnol*. 2004; 22: 1282-9.
- Whitaker GM, Angoli D, Nazzari H, Shigemoto R, Accili EA. HCN2 and HCN4 isoforms self-assemble and co-assemble with equal preference to form functional pacemaker channels. *J Biol Chem*. 2007; 282: 22900-9.
- Xiao J, Yang B, Lin H, Lu Y, Luo X, Wang Z. Novel approaches for gene-specific interference via manipulating actions of microRNAs: examination on the pacemaker channel genes HCN2 and HCN4. *J Cell Physiol*. 2007; 212: 285-92.
- Ye B, Nerbonne JM. Proteolytic processing of HCN2 and co-assembly with HCN4 in the generation of cardiac pacemaker channels. *J Biol Chem*. 2009; 284: 25553-9.
- Plotnikov AN, Sosunov EA, Qu J, Shlapakova IN, Anyukhovskiy EP, Liu L, et al. Biological pacemaker implanted in canine left bundle branch provides ventricular escape rhythms that have physiologically acceptable rates. *Circulation*. 2004; 109: 506-12.
- Qu J, Plotnikov AN, Danilo P, Jr., Shlapakova I, Cohen IS, Robinson RB, et al. Expression and function of a biological pacemaker in canine heart. *Circulation*. 2003; 107: 1106-9.
- Kuck KH, Schluter M, Geiger M, Siebels J, Duckeck W. Radiofrequency current catheter ablation of accessory atrioventricular pathways. *Lancet*. 1991; 337: 1557-61.
- Zhang M, Methot D, Poppa V, Fujio Y, Walsh K, Murry CE. Cardiomyocyte grafting for cardiac repair: graft cell death and anti-death strategies. *J Mol Cell Cardiol*. 2001; 33: 907-21.